

Determination of the Reflectivity of Liquid Semiconductors Over a Wide Temperature Range¹

R. Černý,^{2,3} P. Příkryl,⁴ K. M. A. El-Kader,⁵ and V. Cháb⁵

A new method for the determination of the reflectivity of liquid semiconductors in the temperature range from the melting point to the boiling point is presented in the paper. The method is based on the pulsed laser irradiation of the semiconductor surface, the time-resolved reflectivity (TRR) measurement technique, and the numerical simulation of the process using a nonequilibrium thermal model. Matching the experimental and computed values of the maximum reflectivity of the cw probe laser and the surface melt duration in the dependence on energy density of the laser pulse and a least-squares-based fitting procedure lead to the determination of the reflectivity of the liquid at the wavelength of the primary laser beam. The method is illustrated by experimental data on XeCl (308-nm) and ArF (193-nm) excimer laser irradiation of Si(100), giving the results $B_1 = 0.67 \pm 0.01 - (8 \pm 1) \times 10^{-5} (T-1687)$ at 308 nm and $R_1 = 0.755 \pm 0.010 - (7 \pm 1) \times 10^{-5} (T-1687)$ at 193 nm, where R_1 is the reflectivity of the liquid and T is temperature in K.

KEY WORDS: liquid semiconductors; melting; molten materials; pulsed laser; reflectivity.

1. INTRODUCTION

The reflectivity of liquid semiconductors has been a subject of systematic study only rarely until now. Probably, the first measurements of the optical constants n and k of liquid silicon (l-Si) over a wide frequency range

¹ Paper presented at the Twelfth Symposium on Thermophysical Properties, June 19–24, 1994, Boulder, Colorado, U.S.A.

² Department of Physics, Faculty of Civil Engineering, Czech Technical University, Thákurova 7, 16629 Prague 6, Czech Republic.

³ To whom correspondence should be addressed.

⁴ Mathematical Institute, Czech Academy of Sciences, Žitná 25, 11567 Prague 1, Czech Republic.

⁵ Institute of Physics, Czech Academy of Sciences, Na Slovance 2, 18040 Prague 8, Czech Republic.

(400–1000 nm) were made by Shvarev et al. [1] at the melting temperature (MT) only. Later, Jellison and Lowndes [2] determined first the values of n and k of l-Si at 633 nm using time-resolved ellipsometry and then extended [3] the measurements for the continuous frequency range of 334–633 nm. Also, in Refs. 2 and 3, only the effective values of n and k corresponding to the MT were measured. The only extension above the MT in measuring the reflectivity of liquid semiconductors known to us is the paper by Lampert et al. [4], where the reflectivity of Si at 633 nm was determined up to ~ 200 K above the melting point.

In this paper, we developed a new method for the determination of temperature-dependent reflectivity of liquid semiconductors for the primary pulsed laser wavelength using time-resolved reflectivity (TRR) measurements, the known data for the reflectivity of the solid phase, and the known dependencies of the refraction index and the extinction coefficient on temperature for the probe cw laser beam. The method is verified by the experimental data for Si(100) surface irradiated by ArF and XeCl excimer lasers.

2. METHOD FOR DETERMINATION OF $R_l(T)$

We consider the following problem: A semiconductor sample is irradiated by a pulse laser with the energy density E , which is sufficiently high to melt the sample surface. A cw laser focused onto the irradiated spot on the sample surface is used for TRR measurements. As a result of TRR measurements, the experimentally determined functions $R_{\max}^p = R_{\max}^p(E)$ and $t_m = t_m(E)$ can be obtained, where R_{\max}^p is the maximum reflectivity of the probe laser beam, and t_m is the melt duration. Our aim is the determination of the temperature-dependent reflectivity of the liquid at the wavelength of the primary laser light, $R_l(T)$.

Theoretical description of the problem is based on our previously published [5] thermal model of nonequilibrium melting and solidification of semiconductors under pulsed laser irradiation. Using this model we obtain the computer-simulated TRR curves, and consequently the computer equivalents, $R_{\max,c}^p = R_{\max,c}^p(E)$, $t_{m,c} = t_{m,c}(E)$, of experimental curves $R_{\max}^p(E)$, $t_m(E)$. The algorithm for determination of $R_l(T)$ is given below.

2.1. Determination of $R_l(T)$ in the “Transition Zone” on the $R_{\max}^p(E)$ Curve

The transition zone means the region where the influences of the solid and liquid layers are combined, i.e., the maximum thickness Z_{\max} of the liquid layer is smaller than a few absorption lengths of the primary pulsed laser, $Z_{\max} < K/\alpha_l$, where α_l is the mean optical absorption coefficient of the liquid, and K is, typically, 3–5.

The procedure is described as follows.

1. Suppose that $n_s(T), k_s(T)$ are known.
2. Choose the functions $n_l(T), k_l(T)$ in the region near the melting temperature, e.g., $n_l(T) = n_0, k_l(T) = k_0$
3. Choose a set of values $n_{0i}, k_{0i}, i = 1, 2, \dots, n$.
4. Compute $R_{\max,c,i}^p = R_{\max,c,i}^p(E_i)$ for all experimentally given E_i in the transition zone and all n_{0i}, k_{0i} .
5. Compute error limits of $R_{\max,c}^p(E)$ due to the errors in the input parameters of the model.
6. Compute for all the values of n_{0i}, k_{0i} the quantity $LS = 1/N_1^2 \sum_{j=1}^{N_1} [R_{\max,c,j}^p(E_j) - R_{\max,j}^p(E_j)]^2$, where N_1 is the number of experimentally determined values of R_{\max}^p for E_i in the transition zone.
7. Find $LS_{\min} = \min(LS(A_i), i = 1, 2, \dots, n)$, put $n_0 = n_{0,\min}, k_0 = k_{0,\min}$, where $n_{0,\min}, k_{0,\min}$, are the values of n_{0i}, k_{0i} corresponding to the LS_{\min} .
8. Discuss the error bars of $R_{\max,c}^p(E)$ computed with n_0, k_0 , and $R_{\max}^p(E)$. If there are coinciding parts of these two error bars in all range of the energy densities considered, accept n_0, k_0 as the solution of the fitting procedure.
9. Compute the correlation coefficient r as a test of goodness of fit,

$$r = \frac{n \sum_{i=1}^n x_E x_C - \sum_{i=1}^n x_E \sum_{i=1}^n x_C}{\sqrt{[n \sum_{i=1}^n x_E^2 - (\sum_{i=1}^n x_E)^2][n \sum_{i=1}^n x_C^2 - (\sum_{i=1}^n x_C)^2]}} \quad (1)$$

where x_E are the experimental values of R_{\max}^p , x_C are the computed values of $R_{\max,c}^p$, and n is the number of points.

2.2. Determination of $R_l(T)$

For $Z_{\max} > K/\alpha_l$ we can neglect the influence of the solid on the value of reflectivity and take the liquid layer into account only.

1. Choose the $R_l(T)$ function, e.g., $R_l(\bar{T}) = R_{l0} + B(\bar{T} - T_m)$, where \bar{T} is the characteristic temperature defined as $\bar{T}(t) = (\int_0^Z T(x,t) e^{-\alpha x} dx) / (\int_0^Z e^{-\alpha x} dx)$, t is the time, α is the mean optical absorption coefficient of the liquid at the wavelength of the primary laser beam, Z is the thickness of the liquid phase, T_m is the melting temperature, and $R_{l0} = ((n_0 - 1)^2 + k_0^2) / ((n_0 + 1)^2 + k_0^2)$.

2. Choose a set of values B_i , $i = 1, 2, \dots, m$.
3. Compute $t_{m,c} = t_{m,c}(E_i)$ for experimentally given $E_i > E_t$.
4. Compute error limits of $t_{\max,c}(E)$ due to the errors in the input parameters of the model.
5. Compute for all the values of B_i the quantity $LST = 1/N_2 \sum_{j=1}^{N_2} [t_{m,c,j}(E_j) - t_{m,j}(E_j)]^2$; N_2 is the number of experimentally determined values of t_m for $E > E_m$.
6. Find $LST_{\min} = \min(LST(B_i), i = 1, 2, \dots, m)$, and put $B = B_{\min}$, where B_{\min} is the value of B_i corresponding to the LST_{\min} .
7. Discuss the error bars of $t_{\max,c}(E)$ computed with B and $t_{\max}(E)$. If there are coinciding parts of these two error bars in all range of the energy densities considered, accept B as the solution of the fitting procedure.
8. Compute the correlation coefficient r as a test of godness of fit using Eq. (1), where x_E are the experimental values of t_m , and x_C and the computed values of t_m .

3. EXPERIMENTS

In our experiments, we used the experimental setup described in Ref. 6. Samples cut from 0.35-mm-thick wafers of Czochralski-grown, p-type Si(100) single crystals ($5\text{--}12 \Omega \cdot \text{cm}$), with the surface prepared using a standard Syton polish, were irradiated in a UHV chamber by the ArF (193 nm, 10-ns FWHM) and XeCl (308 nm, 27-ns FWHM) excimer lasers.

The error limits of the measurements of $R_{\max}^p \pm 1\%$ were in the solid phase, $\pm 5\%$ in the transition zone, and $\pm 3\%$ in the fully developed liquid phase; the time of melting t_m was measured with a precision of ± 5 ns.

4. RESULTS AND DISCUSSION

The results of our theoretical-experimental treatment can be summarized as follows. ArF laser:

$$R_1 = 0.755 \pm 0.010 - (7 \pm 1) \times 10^{-5}(T - 1687) \quad (2)$$

XeCl laser:

$$R_1 = 0.67 \pm 0.01 - (8 \pm 1) \times 10^{-5}(T - 1687) \quad (3)$$

The points in Fig. 1 represent the maximum values of the reflectivity of the HeNe probe laser for Si, taken from the experimental TRR signals

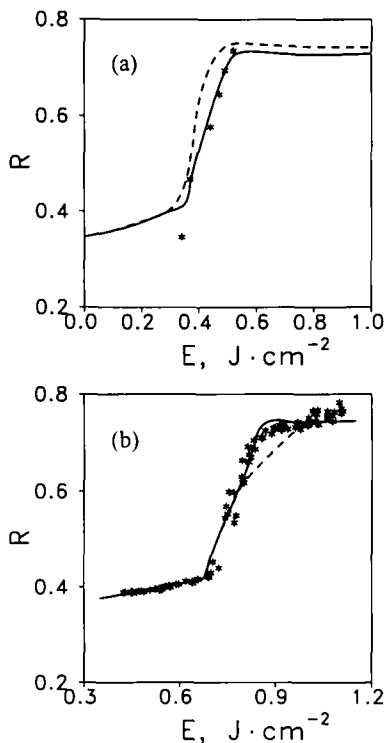


Fig. 1. Maximum reflectivity of Si at the wavelength of HeNe probe laser vs energy density of the (a) ArF laser pulse and (b) XeCl laser pulse calculated using the values of $R_l(T)$ determined by the new fitting procedure (—) and with (a) $R_l = 0.679$ (---) and (b) $R_l = 0.691$ (---). Stars denote experimental points.

as a function of the pulse energy density E for ArF, XeCl lasers. The solid curves are obtained by numerical simulation using the described non-equilibrium model, the reflectivity of the liquid phase at 193 and 308 nm being free parameters in the fitting procedure.

In performing the goodness-of-fit tests, similarly as in the fitting procedure itself, we divided the $R_{max}^p = R_{max}^p(E)$ curves into two regions, the "transition zone" and the fully developed liquid phase. In the transition zone, the correlation coefficient was $r = 0.92$ for the XeCl laser and $r = 0.95$ for the ArF laser. However, the correlation in the region of the fully developed liquid phase was poor, $r = 0.17$ for the XeCl laser and $r = 0.15$

for the ArF laser, which is due to the fact that the data for reflectivity of l-Si at 632.8 nm for $T > T_m$ are not very reliable, and the $R_{\max}^p = R_{\max}^p(E)$ curve is almost a constant in this region, which makes reaching a good correlation more difficult. However, also here the theoretical curves lie within the error bar of experimental measurements, and it should be noted that we do not use this part of the $R_{\max}^p = R_{\max}^p(E)$ curve in our fitting procedure.

Figure 2 shows the values of melt duration of a Si surface in the dependence on the energy density of the pulse. Similarly as in Fig. 1, the solid curves represent the results of our fitting procedure with the reflectivity of liquid silicon as a free parameter.

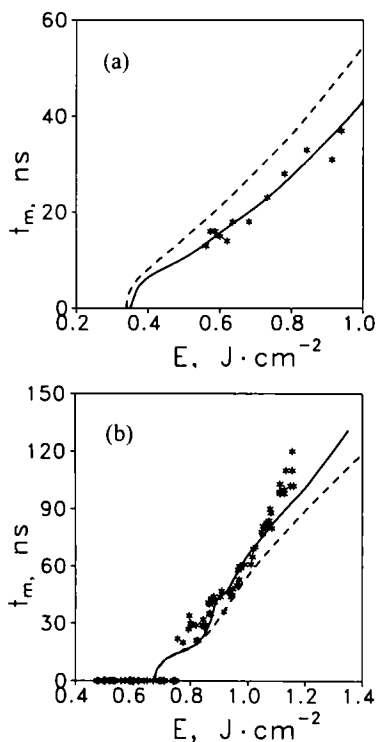


Fig. 2. Melt duration vs energy density of the (a) ArF laser pulse and (b) XeCl laser pulse calculated using the values of $R_l(T)$ determined by the new fitting procedure (—) and with (a) $R_l = 0.679$ (---) and (b) $R_l = 0.691$ (---). Stars denote experimental points.

The goodness-of-fit tests showed a very good correlation of the calculated $t_m(E)$ curves with the experimental data, $r=0.98$ for the XeCl laser and $r=0.99$ for the ArF laser. However, the agreement of experiments with the theoretical $t_m(E)$ curve was good in all the range of energy densities for the ArF laser only. In the case of the XeCl laser, the markedly larger discrepancies were observed at highest energy densities ($>1.2 \text{ Jcm}^{-2}$), where the experimental melting times are systematically longer than those obtained by numerical simulations. Since the theoretical predictions have shown a very good agreement with experiments for all lower energy densities, the probable reason of the observed disagreement might be the higher complexity of the experimental conditions which are not reflected in the theory. At least, the detailed distribution of the energy in a laser pulse and damage of the surface oxide layer can be considered as examples of these additional effects.

Comparison of our computed parameters of the liquid reflectivity with those from other sources shows significant differences. Jellison [7] determined the reflectivity of l-Si for 308 nm at the melting temperature using the extrapolation of the ellipsometric measurements by Shvarev [1] to be 0.734; Unamuno et al. [8] measured the value $R_1=0.691$ for 308 nm. For 193 nm, Unamuno and Fogarassy [9] used the value from their previous measurements [8], $R_1=0.679$; Jellison et al. [10], $R_1=0.781$. It should be noted that in the relation for R_1 , we can compare only the values at the melting temperature. There are neither theoretical nor experimental data, known to us, for the reflectivity of liquid silicon at 193 and 308 nm above the melting temperature.

For the sake of comparison, we used the value $R_1=0.691$ for Si at 308 nm and $R_1=0.679$ for Si at 193 nm, recommended in Refs. 8 and 9, as input parameters of our model, and compared the results with those obtained by our fitting procedure. As shown in Figs. 1 and 2, the value of $R_{\text{max,c}}^p$ computed with R_1 from Refs. 8 and 9 (dashed line in the figures) are outside the error bar of our experimental measurements in most of the transition zone; also, the values of $t_{\text{m,c}}$ computed with R_1 from Refs. 8 and 9 are for a relatively wide range of energies outside the error bar. This supports our claim of the temperature dependence of the reflectivity of l-Si at both 193 and 308 nm.

The computational model we used to simulate numerically the TRR curves is capable of reproducing satisfactorily the experimentally determined melting and evaporation thresholds as well as the melt durations (see Ref. 11), which are the most often measured parameters in laser processing of semiconductors. Therefore, we have good reason to believe that also the temperature fields generated numerically by the model (temperature measuring with the resolutions of 5 nm and 2 ns is not feasible at

present) are calculated with a reasonable precision. Knowing the temperature field provides, then, a good basis for deriving a method for the determination of the reflectivity vs temperature relation at the wavelength of the primary laser beam.

Using the nonequilibrium model of phase-change processes initiated by pulsed-laser irradiation (instead of the commonly used equilibrium models) gives us the opportunity to calculate the overheating and undercooling of the phase interface (see Ref. 5 for details) in a dependence of its velocity. The interface velocity vs temperature relation, which is usually called the "interface response function" (see, e.g., Ref. 12), can be determined either experimentally or by molecular dynamics simulations. In our model, we have used for silicon the analytical relation by Kluge and Ray [13], which was obtained by a molecular dynamics study using the Stillinger-Weber model of silicon [14] and which was shown to be in very good agreement with the experimental measurements by Galvin et al. [15]. Therefore, also here we can consider our calculated values of overheating and undercooling as reasonable.

5. CONCLUSION

The exact calculation of the reflectivity of the silicon sample in the "transition zone" considering the sample to be an optically inhomogeneous medium with continuous variations of the optical parameters in both crystalline and liquid silicon and a jump change in the complex refraction index \hat{n} at the interface between c-Si and l-Si favor the newly developed fitting procedure compared to previous ones.

A simultaneous good agreement between the theoretical and the experimental data for both the $R_{\max}^p(E)$ and the $t_m(E)$ curves was achieved in this paper for the first time. A comparison with the previous attempts in this field (see, e.g., Refs. 11 and 16) shows that this agreement is due to the fact that the temperature dependence of the reflectivity of l-Si at the wavelength of the primary laser beam is taken into account.

ACKNOWLEDGMENT

This paper is based upon work supported by the Grant Agency of the Czech Republic, under Grant 202/93/2383.

REFERENCES

1. K. M. Shvarev, B. A. Baum, and P. V. Geld, *High Temp.* **15**:548 (1977).
2. G. E. Jellison, Jr., and D. H. Lowndes, *Appl. Phys. Lett.* **47**:718 (1985).
3. G. E. Jellison, Jr., and D. H. Lowndes, *Appl. Phys. Lett.* **51**:352 (1987).

4. M. O. Lampert, J. M. Koebel, and P. Siffert, *J. Appl. Phys.* **52**:4975 (1981).
5. R. Černý, R. Šášik, I. Lukeš, and V. Cháb, *Phys. Rev. B* **44**:4097 (1991).
6. D. H. Auston, J. A. Golovchenko, A. L. Simons, C. M. Surko, and C. Venkatesan, *Appl. Phys. Lett.* **34**:777 (1979).
7. G. E. Jellison, Jr., in *Semiconductors and Semimetals, Vol. 23*, R. F. Wood, C. W. White, and R. T. Young, eds. (Academic Press, New York, 1984), p. 95.
8. S. de Unamuno, M. Toulemonde, and P. Siffert, in *Laser Processing and Diagnostics, Vol. 33* (Springer, Berlin, 1984), p. 35.
9. S. de Unamuno and E. Fogarassy, *Appl. Surf. Sci.* **36**:1 (1989).
10. G. F. Jellison, Jr., D. H. Lowndes, D. N. Mashburn, and R. F. Wood, *Phys. Rev. B* **34**:2407 (1986).
11. I. Lukeš, R. Šášik, and R. Černý, *Appl. Phys. A* **54**:327 (1992).
12. R. F. Wood and F. W. Young, Jr., in *Semiconductors and Semimetals, Vol. 23*, R. F. Wood, C. W. White, and R. T. Young, eds. (Academic Press, New York, 1984), p. 252.
13. M. D. Kluge and J. R. Ray, *Phys. Rev. B* **39**:1738 (1989).
14. F. H. Stillinger and T. A. Weber, *Phys. Rev. B* **31**:5162 (1985).
15. G. J. Galvin, J. W. Mayer, and P. S. Percy, *Appl. Phys. Lett.* **46**:644 (1985).
16. D. H. Lowndes and G. E. Jellison, Jr., in *Semiconductors and Semimetals, Vol. 23*, R. F. Wood, C. W. White, and R. T. Young, eds. (Academic Press, New York, 1984), p. 314.